Bifurcation Analysis for the Generalized Nosé–Hoover System

Rizgar H. Salih [ORCID]*
*Department of Mathematics, University of Raparin,
Rania 46012, Iraq*
rizgar.salih@uor.edu.krd

Julien C. Sprott [ORCID]
*Department of Physics, University of Wisconsin,
Madison, WI 53706, USA*
sprott@physics.wisc.edu

Bashdar M. Mohammed [ORCID]
*Department of Mathematics, University of Raparin,
Rania 46012, Iraq*
bashdar.mahmoodmuhamad@uor.edu.krd

This study investigates the generalized Nosé–Hoover system. The original version of the system is a chaotic system designed to represent the interaction between a harmonic oscillator and a heat bath maintained at a constant temperature. Despite its simplicity in just three dimensions, it exhibits complex and unusual dynamics. This investigation focuses on studying local bifurcations, including Saddle-Node and Hopf bifurcations, of the generalized Nosé–Hoover system. In terms of cyclicity, the Lyapunov quantities technique is used to demonstrate that three periodic orbits can bifurcate from the Hopf point. This mathematical research contributes to understanding the equilibrium points, their stability and the dynamics of the nonlinear model when some of the parameters are varied.

Keywords: Nosé–Hoover system; Hopf bifurcation; Saddle-Node bifurcation; limit cycle; Lyapunov quantities.

1. Introduction

Bifurcation theory has deep roots in classical mathematics, including the notable work by L. Euler dating back to 1744. However, its origins can be traced back to Poincaré and his significant contributions to the qualitative analysis of differential equations. This theory focuses on investigation of qualitative alterations within the phase portrait, such as the presence or absence of equilibrium points, periodic solutions and even more intricate phenomena like strange attractors [Euler, 1744].

In this paper, the following system, known as the generalized Nosé–Hoover system, is considered. It was introduced by Sprott.

$$\dot{x}_1 = x_2, \quad \dot{x}_2 = -x_1 + x_2 x_3, \quad \dot{x}_3 = f(x_1, x_2, x_3),$$
$$(1)$$

where $f(x_1, x_2, x_3) = \alpha_0 + \alpha_1 x_1 + \alpha_2 x_2 + \alpha_3 x_3 + \alpha_4 x_1^2 + \alpha_5 x_1 x_2 + \alpha_6 x_1 x_3 + \alpha_7 x_2^2 + +\alpha_8 x_2 x_3 + \alpha_9 x_3^2$

---

*Author for correspondence

and $\alpha_i \in \mathbb{R}$ ($i = 0, \ldots, 9$). Several types of systems, each characterized by at most a single equilibrium point, were partially investigated and studied by him through parameter variations. The results demonstrated the existence of 11 examples of chaotic systems for each of the eight types, alongside one system that lacks any equilibrium points and two nonhyperbolic systems. Moreover, among the 11 cases examined, six showcased hidden chaotic attractors and six exhibited multistability under the specified parameters [Sprott, 2015]. However, it is worth noting that the bifurcation of system (1) has received relatively less attention based on the available knowledge. Here, a further contribution is made to the understanding of the complexity, specifically the topological structure of the dynamics of system (1), by studying the effects of parameter variations. The novelty of this research lies in the focused exploration of local bifurcations, particularly Saddle-Node and Hopf bifurcations, within the generalized Nosé–Hoover system. Through the analysis of these bifurcations, the changes in system behavior are uncovered as key parameters vary, shedding light on the underlying dynamics and transitions between different states.

This paper is organized as follows: Sec. 2 deals with the introduction of the Nosé–Hoover system and its modifications. Section 3 focuses on identifying the existence of equilibrium points in the generalized Nosé–Hoover system and studying their stability. Section 4 is dedicated to the study of the local bifurcation of system (1). It examines the presence of Saddle-Node bifurcation in system (1), along with the conditions for the occurrence of Hopf bifurcations. Furthermore, the Lyapunov quantities technique is applied to investigate the cyclicity of the system and identify bifurcated limit cycles stemming from the Hopf points. Lastly, the conclusions that have been reached are presented.

2. The Nosé–Hoover System with Its Modifications

The Nosé–Hoover system, widely recognized as a conservative system, has received significant attention in research. In a groundbreaking publication from 1984, Nosé [1984a, 1984b] introduced a set of equations that revolutionized the field of thermodynamics, establishing a new paradigm. Posch *et al.* made the Nosé equations simpler in 1986 by eliminating an unnecessary variable and substituting

the remaining "momentum" with a "friction" coefficient. As a result, they derived the equations of motion for the Nosé–Hoover system as follows:

$$\dot{x}_1 = x_2, \quad \dot{x}_2 = -x_1 - x_2 x_3,$$
$$\dot{x}_3 = \alpha(x_2^2 - 1), \tag{2}$$

x_1 represents the coordinate of the oscillator, x_2 symbolizes momentum, x_3 denotes the friction coefficient and α assumes the role of a positive coupling parameter. They investigated the dynamics of system (2), employing Lyapunov exponents and Poincaré phase space sections. They found various periodic orbits and KAM tori for certain α values. Higher α values led to a mix of regular and chaotic solutions, with stable islands which are surrounded by a chaotic sea. The fractal dimension and Lyapunov instability of the chaotic regimes were also examined in their analysis [Posch *et al.*, 1986]. This system has subsequently been investigated by researchers from various fields, resulting in diverse findings. Presented below are some notable contributions. The system was examined by [Hoover, 1985] for different fixed values of the parameter α, revealing its rich dynamics characterized by a combination of regular and chaotic trajectories in phase space. The investigation of periodic orbits in the system was later undertaken by Swinnerton-Dyer and Wagenknecht. In their paper, two notable approaches to the theory of Nosé–Hoover equations were mentioned: one involves the study of trajectories for small α, while the other centers around the examination of trajectories approaching infinity. The existence of several types of periodic orbits of system (2) for $0 < \alpha \leq 1$ was demonstrated by the authors using the second possible approach, as shown in [Swinnerton-Dyer & Wagenknecht, 2008]. These orbits bifurcate from heteroclinic orbits to equilibrium points at infinity [Swinnerton-Dyer & Wagenknecht, 2008]. Next, Mahdi and Valls examined the integrability of system (2). They showed that the system has no polynomial first integrals, Darboux first integrals and Darboux polynomial with nonzero cofactors. They also proved that the system has two exponential factors e^{x_2} and $e^{x_3^2 + \alpha(x_1^2 + x_2^2)}$ with cofactors x_1 and $-2\alpha x_3$, respectively. Moreover, they proved that the system is integrable when $\alpha = 0$ [Mahdi & Valls, 2011]. Subsequently, Wang and Yang [2015] revisited the system with a fixed parameter $\alpha = 10$ and presented numerous novel and remarkable dynamical phenomena through numerical analysis. Lastly,

an investigation into the time-reversible dynamics of the system was conducted by Deng *et al.* in order to reveal its intricate pathway for generating non-trivial chaos. The spectrum of Lyapunov exponents, predictability and fractal dimension of both forward and backward chaotic attractors were examined by them. However, despite their efforts, no recognized form of chaos that could account for the findings was identified [Deng *et al.*, 2023a]. In [Li *et al.*, 2022], researchers investigated the integrability and nonintegrability of system (2).

Based on system (2), Hoover [2007] created the following system:

$$\dot{x}_1 = x_2, \quad \dot{x}_2 = -x_1 - x_2 x_3,$$
$$\dot{x}_3 = x_2^2 - 1 - \epsilon \tanh(x_1). \tag{3}$$

Many interesting and surprising dynamic behaviors were demonstrated by Sprott and his co-author as follows. For certain values of ϵ, it was found that conservative regions can coexist with dissipative regions in phase space by constructing an appropriate cross-section. In particular, it was shown that the generalized oscillator possesses interlinked invariant tori [Sprott *et al.*, 2014]. Rech has modified system (3) by multiplying a parameter α to the $\dot{x}_3$ equation. Through the application of Lyapunov exponents, the researchers analyzed the model's behavior across various parameter values. Their findings revealed the existence of dissipative quasiperiodic structures within a chaotic region [Rech, 2016].

The following two simple three-dimensional autonomous chaotic systems were described by Munmuangsaen *et al.* to make system (2) dissipative:

$$\dot{x}_1 = x_2 + b x_1, \quad \dot{x}_2 = x_2 x_3 - x_1,$$
$$\dot{x}_3 = a - x_2^2, \tag{4}$$

$$\dot{x}_1 = x_2, \quad \dot{x}_2 = x_2 x_3 - x_1,$$
$$\dot{x}_3 = a - x_2^2 - b x_3. \tag{5}$$

In general, the analysis of one of the systems includes the examination of various aspects, such as the eigenvalues of the Jacobian matrix, coexisting attractors, the Kaplan–Yorke dimension and bifurcations of the largest Lyapunov exponent [Munmuangsaen *et al.*, 2015].

Wang and Yang modified system (2) by adding an extra term in the third equation, which is defined as follows:

$$\dot{x}_1 = x_2, \quad \dot{x}_2 = -x_1 - x_2 x_3,$$
$$\dot{x}_3 = \alpha(x_1^2 + x_2^2 - 1), \tag{6}$$

where α is a positive parameter. Based on numerical simulations, it was demonstrated that a "fat fractal" structure can be exhibited by this modified system, along with the coexistence of invariant tori and a topological horseshoe [Wang & Yang, 2017]. In [Wang & Yang, 2018], the system was analytically investigated, revealing that a two-dimensional bounded unit disk is traversed infinitely many times by almost all trajectories. Furthermore, it was shown that almost all trajectories have at least one ω-limiting point [Wang & Yang, 2018]. The integrability and nonintegrability of system (6) have been discussed in [Li *et al.*, 2022].

The investigation of system (2) in the following form was carried out by Messias and Retinol:

$$\dot{x}_1 = x_2, \quad \dot{x}_2 = -x_1 - x_2 x_3, \quad \dot{x}_3 = x_2^2 - a, \tag{7}$$

where $a \in \mathbb{R}$. It is dynamically identical to system (2) under the transformation $(x_1, x_2) \rightarrow (A x_1, A x_2)$, where $A^2 = a$. They have proven that the new system, when $a \neq 0$, does not possess invariant algebraic surfaces or polynomial first integrals. Furthermore, the existence of a linearly stable periodic orbit is shown, which bifurcates from a nonisolated zero-Hopf equilibrium point located at the origin when $a > 0$ [Messias & Reinol, 2018]. Cândido and Llibre [2018] have proven that when $a = 0$, system (7) exhibits a zero-Hopf bifurcation. Furthermore, it was demonstrated by Mehrabbeik and her co-authors that by adding an anti-damping term $b x_3$ to the third equation of system (7), the new system exhibits an attracting torus across a wide range of parameter values. Various dynamic solutions, such as limit cycles, strange attractors, attracting tori, invariant tori and a chaotic sea, are encompassed by this system [Mehrabbeik *et al.*, 2022].

The following two simple kinds of system (2) were described by Sprott:

$$\dot{x}_1 = x_2, \quad \dot{x}_2 = -x_1 - a x_2 x_3,$$
$$\dot{x}_3 = x_2^2 - 1, \tag{8}$$

$$\dot{x}_1 = x_2, \quad \dot{x}_2 = -x_1 - a x_2 \, \mathrm{sgn}(x_3),$$
$$\dot{x}_3 = x_2^2 - 1. \tag{9}$$

System (8) is dynamically identical to system (2) under the transformation $x_3 \to \frac{x_3}{a}$ and it precisely satisfies the original goal. Meanwhile, the second one is a bang-bang controller that is conservative and ergodic with a chaotic sea that fills all of phase space with a Gaussian measure for $a > 1.7$ [Sprott, 2018].

System (2) was modified by Libra *et al.* as follows:

$$\dot{x}_1 = x_2 - ax_1x_3, \quad \dot{x}_2 = x_1,$$
$$\dot{x}_3 = b\,(x_1^2 - 1), \tag{10}$$

where a and b are real parameters. The dynamics of the system were globally studied and a comprehensive description of the solutions in the phase space, including the dynamics at infinity via the Poincaré compactification, was provided [Llibre *et al.*, 2021].

Cang *et al.* [2022] extended system (2) as follows:

$$\dot{x}_1 = -ax_1 + x_2x_3,$$
$$\dot{x}_2 = -bx_2 + x_3(x_2 - x_1), \tag{11}$$
$$\dot{x}_3 = k - x_2^2,$$

where $a \geq 0$ and $b,\ k \in \mathbb{R}$. They demonstrated that the system exhibits various dynamic behaviors, including Saddle-Node bifurcation, fold-Hopf bifurcation, transient and conservative chaos.

Deng *et al.* defined the following three-dimensional system:

$$\dot{x}_1 = x_2, \quad \dot{x}_2 = -x_1 - x_2x_3,$$
$$\dot{x}_3 = \alpha(x_2^2 - 1 - \epsilon x_3). \tag{12}$$

This system is derived from system (5) through the transformation $(x_1, x_2, x_3) \to (\sqrt{a}x_1, \sqrt{a}x_2, x_3)$, where $\epsilon = \frac{b}{a}$. The chaotic dynamics of the model were numerically characterized by utilizing the maximum Lyapunov exponent. It was shown that, with higher values of the new dissipative parameter ϵ, the prevalence of chaotic behavior is observed only in the backwards dynamics [Deng *et al.*, 2023b]. The generalized Nosé–Hoover system (1), which is introduced by [Sprott, 2015], is a version of the system.

3. Existence and Stability of Equilibrium Points

The foundational building blocks for various aspects within dynamical systems are provided by equilibrium points. To determine the equilibrium points of system (1), the right-hand sides of the equations are set to zero:

$$x_2 = 0,$$
$$-x_1 + x_2x_3 = 0,$$
$$\alpha_0 + \alpha_1x_1 + \alpha_2x_2 + \alpha_3x_3 + \alpha_4x_1^2$$
$$\quad + \alpha_5x_1x_2 + \alpha_6x_1x_3 + \alpha_7x_2^2 + \alpha_8x_2x_3$$
$$\quad + \alpha_9x_3^2 = 0. \tag{13}$$

When the values of $x_2 = 0$ and $x_1 = 0$ are substituted into Eq. (13), it transforms into

$$\alpha_9x_3^2 + \alpha_3x_3 + \alpha_0 = 0, \tag{14}$$

its roots are $x_3 = \frac{-\alpha_3 + \sqrt{\Delta}}{2\alpha_9}$, where $\Delta = \alpha_3^2 - 4\alpha_9\alpha_0$. It is assumed that the real root $x_3 = x_3^*$ of Eq. (14) represents the equilibrium point $(0, 0, x_3^*)$ of system (1), which is situated on the x_3-axis.

- When $\Delta < 0$, Eq. (14) does not have any real solutions. As a consequence, system (13) lacks real roots, indicating the absence of an equilibrium point in the system.
- When $\Delta > 0$,
  - (i) If $\alpha_9 \neq 0$, then $E_1^{\pm} = (0, 0, \frac{-\alpha_3 \pm \sqrt{\Delta}}{2\alpha_9})$ represents two equilibrium points of the system.
  - (ii) If $\alpha_9 = 0$ and $\alpha_3 \neq 0$, then $E_2 = (0, 0, -\frac{\alpha_0}{\alpha_3})$ represents a line of singularity of the system.
- When $\Delta = 0$,
  - (i) If $\alpha_9 \neq 0$, then $E_3 = (0, 0, -\frac{\alpha_3}{2\alpha_9})$ represents a single equilibrium point of the system.
  - (ii) If $\alpha_9 = \alpha_3 = 0$ and $\alpha_0 \neq 0$, then the system does not possess any equilibrium point.
  - (iii) If $\alpha_9 = \alpha_3 = \alpha_0 = 0$, then $(0, 0, x_3)$ represents a line of equilibrium of the system.

Proposition 1. *For system (1) with $\Delta = \alpha_3^2 - 4\alpha_9\alpha_0$.*

- (I) *The equilibrium point E_1^+ is always unstable, while E_1^- is asymptotically stable if and only if $\frac{2\alpha_9\sqrt{\Delta} + \sqrt{\Delta} + \alpha_3}{2\alpha_9} > 0$ and $(2\alpha_9\sqrt{\Delta} + \sqrt{\Delta} + \alpha_3)(\alpha_9\sqrt{\Delta} + \Delta + 2\alpha_9) > 4\alpha_9^2\sqrt{\Delta}$.*
- (II) *If $\alpha_3 > 0$, the equilibrium point E_2 is unstable, whereas it is asymptotically stable if and only if $\alpha_3 < 0$, $\alpha_0 < \alpha_3^2$ and $(\alpha_0 - \alpha_3^2)(1 - \alpha_0) < -\alpha_3^2$.*
- (III) *When $\frac{\alpha_3}{2\alpha_9} < 0$ or $\frac{\alpha_3}{2\alpha_9} > 0$, the point E_3 is an unstable nonhyperbolic equilibrium point.*

Proof. The following expression represents the Jacobian matrix of system (1) evaluated at the point $(0, 0, x_3^*)$:

$$J(x_3^*) = \begin{pmatrix} 0 & 1 & 0 \\ -1 & x_3^* & 0 \\ \alpha_6 x_3^* + \alpha_1 & \alpha_8 x_3^* + \alpha_2 & 2\alpha_9 x_3^* + \alpha_3 \end{pmatrix},$$

and the characteristic equation is given by

$$\lambda^3 - (2\alpha_9 x_3^* + x_3^* + \alpha_3)\lambda^2$$
$$- (2\alpha_9 x_3^{*2} + \alpha_3 x_3^* + 1)\lambda$$
$$- (2\alpha_9 x_3^* + \alpha_3) = 0. \quad (15)$$

(I) When $x_3^* = \frac{-\alpha_3 \pm \sqrt{\Delta}}{2\alpha_9}$, Eq. (15) becomes

$$\lambda^3 - \frac{2\alpha_9(\pm\sqrt{\Delta}) + (\pm\sqrt{\Delta}) - \alpha_3}{2\alpha_9}\lambda^2$$
$$- \frac{\alpha_3(\pm\sqrt{\Delta}) - \Delta - 2\alpha_9}{2\alpha_9}\lambda - (\pm\sqrt{\Delta}) = 0. \quad (16)$$

At the equilibrium E_1^+, when the determinant of the Jacobian matrix is $\sqrt{\Delta} > 0$, it implies that at least one of the eigenvalues is positive. Then, the equilibrium point E_1^+ is unstable [see Fig. 1(a)]. At the equilibrium point E_1^-, by comparing Eq. (15) with Eq. (22), we find that $T = -\frac{2\alpha_9\sqrt{\Delta} + \sqrt{\Delta} + \alpha_3}{2\alpha_9}$, $K = -\frac{\alpha_3\sqrt{\Delta} + \Delta + 2\alpha_9}{2\alpha_9}$ and $D = -\sqrt{\Delta}$. By Hurwitz's Theorem, the equilibrium point E_1^- is asymptotically stable if and only if $\frac{2\alpha_9\sqrt{\Delta} + \sqrt{\Delta} + \alpha_3}{2\alpha_9} > 0$ and $(2\alpha_9\sqrt{\Delta} + \sqrt{\Delta} + \alpha_3)(\alpha_9\sqrt{\Delta} + \Delta + 2\alpha_9) > 4\alpha_9^2\sqrt{\Delta}$ [see Fig. 1(b)].

(II) When $\alpha_9 = 0$ and $x_3^* = -\frac{\alpha_0}{\alpha_3}$, the characteristic equation (15) is

$$\lambda^3 + \frac{\alpha_0 - \alpha_3^2}{\alpha_3}\lambda^2 + (1 - \alpha_0)\lambda - \alpha_3 = 0. \quad (17)$$

From Eq. (17), we can deduce that the determinant of the Jacobian matrix is represented by α_3. When $\alpha_3 > 0$, this indicates that at least one of the eigenvalues is positive. Thus, the equilibrium point E_2 is unstable [see Fig. 2(a)]. However, by Hurwitz's Theorem, E_2 is asymptotically stable equilibrium point if and only if $\alpha_3 < 0$, $\alpha_0 < \alpha_3^2$ and $(\alpha_0 - \alpha_3^2)(1 - \alpha_0) < -\alpha_3^2$ [see Fig. 2(b)].

(III) When $\alpha_0 = \frac{\alpha_3^2}{4\alpha_9}$ and $x_3^* = -\frac{\alpha_3}{2\alpha_9}$, the characteristic equation (15) can be written of the form

$$\lambda\left(\lambda^2 + \frac{\alpha_3}{2\alpha_9}\lambda + 1\right) = 0. \quad (18)$$
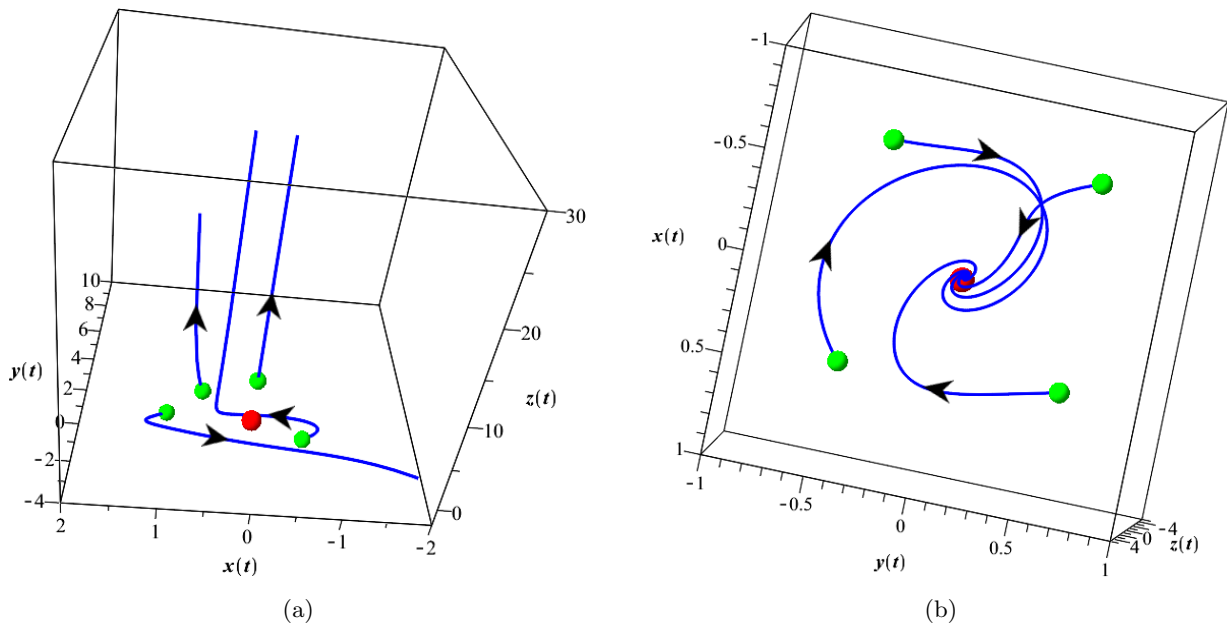

| (a) | (b) |

Fig. 1. The phase portrait of system (1) is shown when $\alpha_i = 1(i = 1, \ldots, 9)$ and $\alpha_0 = 0$. In (a), E_1^+ is unstable and in (b), E_1^- is asymptotically stable. The green balls represent the initial points, while the red balls represent the equilibrium points.
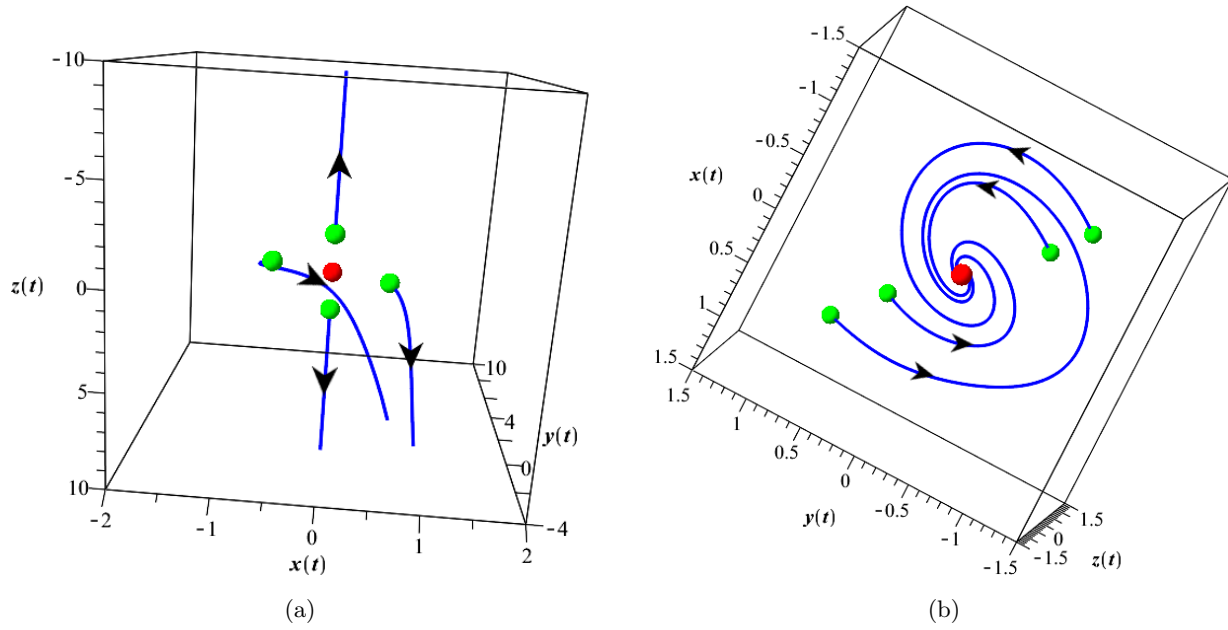
Fig. 2.   The phase portrait of system (1) is shown when $\alpha_1 = \alpha_2 = \alpha_4 = \alpha_5 = \alpha_6 = \alpha_7 = \alpha_8 = \alpha_9 = 1$. (a) When $\alpha_0 = \alpha_3 = 1$, E_2 is unstable. (b) When $\alpha_0 = \alpha_3 = -1$, E_2 is asymptotically stable. The green and red balls indicate the initial and equilibrium points, respectively.
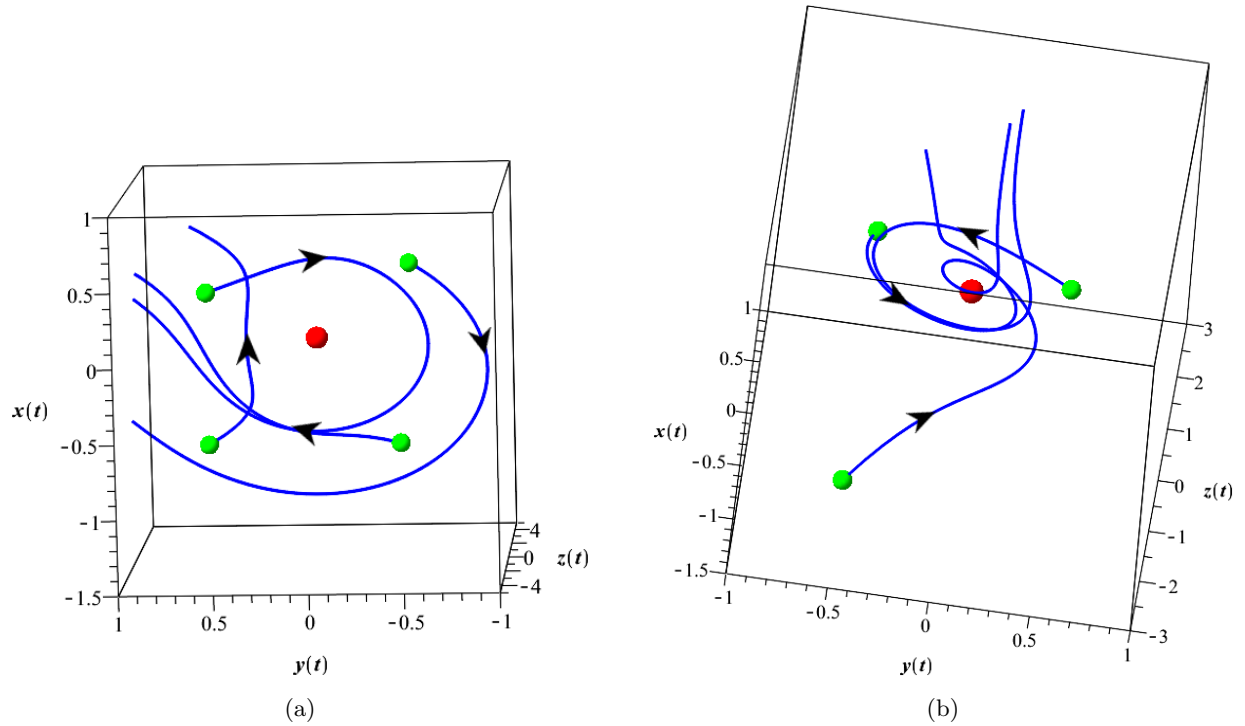

Fig. 3.   The phase portrait of system (1) is shown when $\alpha_1 = \alpha_2 = \alpha_4 = \alpha_5 = \alpha_6 = \alpha_7 = \alpha_8 = \alpha_9 = 1$ and $\alpha_0 = \frac{1}{4}$. (a) When $\alpha_3 = 1$ and (b) $\alpha_3 = -1$ the equilibrium point E_3 is unstable. The green and red balls indicate the initial and equilibrium points, respectively.

From Eq. (18),

- When $\frac{\alpha_3}{2\alpha_9} < 0$, it guarantees the existence of a root that is either positive or has a positive real component. Thus, the equilibrium point E_3 is unstable [see Fig. 3(a)].
- When $\frac{\alpha_3}{2\alpha_9} > 0$, the two nonzero roots exhibit negativity or negative real components. As a result, the overall stability of the equilibrium point depends on how the dynamics behave on the center manifold. By scaling $x_3 \to x_3 - \frac{\alpha_3}{2\alpha_9}$ and the following transformation:

$$x_1 = v + \frac{2\alpha_9}{\sqrt{\Delta_1}}w, \quad x_2 = \frac{\Delta_1 - \alpha_3\sqrt{\Delta_1}}{4\alpha_9\sqrt{\Delta_1}}v + \frac{\alpha_3\alpha_9 + 2\sqrt{\Delta_1}}{2\alpha_9\sqrt{\Delta_1}}w, \quad x_3 = u + \zeta_1 v + \zeta_2 w,$$

where

$$\Delta_1 = \alpha_3^2 - 16\alpha_9^2,$$

$$\zeta_1 = \frac{1}{8\alpha_9^2\sqrt{\Delta_1}}((\alpha_3^2\alpha_6 - 2\alpha_3\alpha_9\alpha_1 - 4\alpha_3\alpha_9\alpha_8 + 8\alpha_2\alpha_9^2)\sqrt{\Delta_1} - (2\alpha_9\alpha_1 - \alpha_6\alpha_3)\Delta_1),$$

$$\zeta_2 = \frac{1}{4\alpha_9^2\sqrt{\Delta_1}}((2\alpha_9^2\alpha_1 - \alpha_6\alpha_3\alpha_9)\sqrt{\Delta_1} + 8\alpha_2\alpha_9^3 + 2\alpha_3^2\alpha_6\alpha_9 - 2\alpha_9^2\alpha_3\alpha_1 - 4\alpha_9^2\alpha_3\alpha_8),$$

system (1) is transformed to the following canonical form:

$$\dot{u} = \alpha_9 u^2 + \varphi_1 v^2 + \varphi_2 w^2 + \varphi_3 uv + \varphi_4 uw + \varphi_5 vw + O(3),$$

$$\dot{v} = \frac{-\alpha_3 + \sqrt{\Delta_1}}{4\alpha_9}v + \varphi_6 v^2 + \varphi_7 w^2 + \varphi_8 uv + \varphi_9 uw + \varphi_{10} vw + O(3),$$

$$\dot{w} = \frac{-\alpha_3 - \sqrt{\Delta_1}}{4\alpha_9}w + \frac{\sqrt{\Delta_1}}{2\alpha_9}(\varphi_6 v^2 + \varphi_7 w^2 + \varphi_8 uv + \varphi_9 uw + \varphi_{10} vw) + O(3),$$

(19)

where

$$\varphi_1 = \frac{1}{32\alpha_9^3}(4\alpha_1^2\alpha_3^2\alpha_9^2 + 32\alpha_1\alpha_8\alpha_9^3 + \alpha_6^2\alpha_3^4 - 32\alpha_1^2\alpha_9^4 + 32\alpha_2^2\alpha_9^4 + 32\alpha_1^2\alpha_9^3 + 32\alpha_4\alpha_9^3 - 32\alpha_7\alpha_9^3$$

$$+ 8\sqrt{\Delta_1}\alpha_2\alpha_8\alpha_9^2 - 4\sqrt{\Delta_1}\alpha_3\alpha_8^2\alpha_9 - 4\sqrt{\Delta_1}\alpha_3\alpha_7\alpha_9 + 4\sqrt{\Delta_1}\alpha_3\alpha_6^2\alpha_9 - 8\alpha_1\alpha_2\alpha_3\alpha_9^2 + 4\alpha_1\alpha_3^3\alpha_8\alpha_9$$

$$- 40\alpha_1\alpha_3\alpha_6\alpha_9^2 + 4\alpha_2\alpha_3^2\alpha_6\alpha_9 - 8\alpha_2\alpha_3\alpha_8\alpha_9^2 - 32\alpha_3\alpha_6\alpha_8\alpha_9^2 - 16\alpha_1\alpha_2\alpha_3\alpha_9^3 - 4\alpha_1\alpha_3^3\alpha_6\alpha_9$$

$$+ 8\alpha_1\alpha_3^2\alpha_8\alpha_9^2 + 32\alpha_1\alpha_3\alpha_6\alpha_9^3 + 8\alpha_2\alpha_3^2\alpha_6\alpha_9^2 - 32\alpha_2\alpha_3\alpha_8\alpha_9^3 - 4\alpha_3^3\alpha_6\alpha_8\alpha_9 + 4\sqrt{\Delta_1}\alpha_1^2\alpha_3\alpha_9^2$$

$$- 16\sqrt{\Delta_1}\alpha_1\alpha_2\alpha_9^3 + 8\sqrt{\Delta_1}\alpha_1\alpha_2\alpha_9^2 - 8\sqrt{\Delta_1}\alpha_1\alpha_6\alpha_9^2 + 2\sqrt{\Delta_1}\alpha_3^2\alpha_6\alpha_8 + 8\alpha_3^2\alpha_8^2\alpha_9^2 - 2\alpha_3^3\alpha_6\alpha_8$$

$$+ 4\alpha_3^2\alpha_7\alpha_9 - 8\alpha_3^2\alpha_6^2\alpha_9^2 + 32\alpha_2\alpha_6\alpha_9^3 + 12\alpha_3^2\alpha_6^2\alpha_9 + 4\alpha_3^2\alpha_8^2\alpha_9 + 8\sqrt{\Delta_1}\alpha_5\alpha_9^2 + \sqrt{\Delta_1}\alpha_3^3\alpha_6^2 - 8\alpha_3\alpha_5\alpha_9^2$$

$$- 4\sqrt{\Delta_1}\alpha_1\alpha_3^2\alpha_6\alpha_9 - 4\sqrt{\Delta_1}\alpha_2\alpha_3\alpha_6\alpha_9 + 8\sqrt{\Delta_1}\alpha_1\alpha_3\alpha_8\alpha_9^2 - 4\sqrt{\Delta_1}\alpha_1\alpha_3\alpha_8\alpha_9 - 4\sqrt{\Delta_1}\alpha_3^2\alpha_6\alpha_8\alpha_9$$

$$+ 8\sqrt{\Delta_1}\alpha_2\alpha_3\alpha_6\alpha_9^2),$$

$$\varphi_2 = \frac{-1}{8\alpha_9\Delta_1}(-4\sqrt{\Delta_1}\alpha_3^2\alpha_6\alpha_8\alpha_9 - 4\sqrt{\Delta_1}\alpha_1\alpha_3\alpha_8\alpha_9 - 4\sqrt{\Delta_1}\alpha_2\alpha_3\alpha_6\alpha_9 + 16\alpha_1\alpha_2\alpha_3\alpha_9^3 + 4\alpha_1\alpha_3^3\alpha_6\alpha_9$$

$$- 8\alpha_1\alpha_3^2\alpha_8\alpha_9^2 - 32\alpha_1\alpha_3\alpha_6\alpha_9^3 - 8\alpha_2\alpha_3^2\alpha_6\alpha_9^2 + 32\alpha_2\alpha_3\alpha_8\alpha_9^3 + 4\alpha_3^3\alpha_6\alpha_8\alpha_9 + 8\alpha_1\alpha_2\alpha_3\alpha_9^2$$

$$- 4\alpha_1\alpha_3^2\alpha_8\alpha_9 + 40\alpha_1\alpha_3\alpha_6\alpha_9^2 - 4a_2\alpha_3^2\alpha_6\alpha_9 + 8\alpha_2\alpha_3\alpha_8\alpha_9^2 + 32\alpha_3\alpha_6\alpha_8\alpha_9^2 + 4\sqrt{\Delta_1}\alpha_1^2\alpha_3\alpha_9^2$$

$$- 16\sqrt{\Delta_1}\alpha_1\alpha_2\alpha_9^3 + 8\sqrt{\Delta_1}\alpha_1\alpha_2\alpha_9^2 - 8\sqrt{\Delta_1}\alpha_1\alpha_6\alpha_9^2 + 8\sqrt{\Delta_1}\alpha_2\alpha_8\alpha_9^2 + 2\sqrt{\Delta_1}\alpha_3^2\alpha_6\alpha_8$$

$$+ 4\sqrt{\Delta_1}\alpha_3\alpha_6^2\alpha_9 - 4\sqrt{\Delta_1}\alpha_3\alpha_8^2\alpha_9 - 4\sqrt{\Delta_1}\alpha_3\alpha_7\alpha_9 - \alpha_6^2\alpha_3^4 - 4\sqrt{\Delta_1}a_1\alpha_3^2\alpha_6\alpha_9 + 8\sqrt{\Delta_1}\alpha_1\alpha_3\alpha_8\alpha_9^2$$

$$+ 8\sqrt{\Delta_1}\alpha_2\alpha_3\alpha_6\alpha_9^2 - 4\alpha_1^2\alpha_3^2\alpha_9^2 + 8\alpha_3^2\alpha_6^2\alpha_9^2 - 8\alpha_3^2\alpha_8^2\alpha_9^2 - 32\alpha_1\alpha_8\alpha_9^3 - 32\alpha_2\alpha_6\alpha_9^3 + 2\alpha_3^3\alpha_6\alpha_8$$

$$- 12\alpha_3^2\alpha_6^2\alpha_9 - 4\alpha_3^2\alpha_8^2\alpha_9 - 4\alpha_3^2\alpha_7\alpha_9 + 8\alpha_3\alpha_5\alpha_9^2 + \sqrt{\Delta_1}\alpha_3^3\alpha_6^2 + 8\sqrt{\Delta_1}\alpha_5\alpha_9^2 + 32\ \alpha_1^2\alpha_9^4 - 32\alpha_2^2\alpha_9^4$$

$$- 32\alpha_1^2\alpha_9^3 - 32\alpha_4\alpha_9^3 + 32\alpha_7\alpha_9^3),$$

$$\varphi_3 = \frac{1}{8\alpha_9^2}(4\sqrt{\Delta_1}\alpha_1\alpha_9^2 - 2\sqrt{\Delta_1}\alpha_3\alpha_6\alpha_9 + 4\alpha_1\alpha_3\alpha_9^2 - 16\alpha_2\alpha_9^3 - 2\alpha_3^2\alpha_6\alpha_9 + 8\alpha_3\alpha_8\alpha_9^2 - 2\sqrt{\Delta_1}\alpha_1\alpha_9$$

$$+ \sqrt{\Delta_1}\alpha_3\alpha_6 - 2\sqrt{\Delta_1}\alpha_8\alpha_9 + 2\alpha_1\alpha_3\alpha_9 - \alpha_3^2\alpha_6 + 2\alpha_3\alpha_8\alpha_9 - 8\alpha_6\alpha_9^2),$$

$$\varphi_4 = \frac{-1}{4\alpha_9\Delta_1}(4\sqrt{\Delta_1}\alpha_1\alpha_3\alpha_9^2 - 16\sqrt{\Delta_1}\alpha_2\alpha_9^3 - 2\sqrt{\Delta_1}\alpha_3^2\alpha_6\alpha_9 + 8\sqrt{\Delta_1}\alpha_3\alpha_8\alpha_9^2 - 4\alpha_1\alpha_3^2\alpha_9^2 + 64\alpha_1\alpha_9^4$$

$$+ 2\alpha_3^3\alpha_6\alpha_9 - 32\alpha_3\alpha_6\alpha_9^3 + 2\sqrt{\Delta_1}\alpha_1\alpha_3\alpha_9 - \sqrt{\Delta_1}\alpha_3^2\alpha_6 + 2\sqrt{\Delta_1}\alpha_3\alpha_8\alpha_9 - 8\sqrt{\Delta_1}\alpha_6a_9^2 + 2\alpha_3^2\alpha_1\alpha_9$$

$$- 32\alpha_1\alpha_9^3 - \alpha_3^3\alpha_6 + 2\alpha_3^2\alpha_8\alpha_9 + 16\alpha_6\alpha_3\alpha_9^2 - 32\ \alpha_8\alpha_9^3),$$

$$\varphi_5 = \frac{1}{8\alpha_9^3\sqrt{\Delta_1}}(32\alpha_9^5\alpha_1^2 - 16\alpha_1\alpha_2\alpha_3\alpha_9^4 + 8\alpha_1\alpha_3^2\alpha_8\alpha_9^3 - 32\alpha_1\alpha_3\alpha_6\alpha_9^4 + 32\alpha_9^5\alpha_2^2 + 8\alpha_2\alpha_3^2\alpha_6\alpha_9^3$$

$$- 32\alpha_2\alpha_3\alpha_8\alpha_9^4 - 4\alpha_3^3\alpha_6\alpha_8\alpha_9^2 + 8\alpha_3^2\alpha_6^2\alpha_9^3 + 8\alpha_3^2\alpha_8^2\alpha_9^3 + 4\alpha_1^2\alpha_3^2\alpha_9^2 - 32\alpha_1^2\alpha_9^4 - 8\alpha_1\alpha_2\alpha_3\alpha_9^3$$

$$- 4\alpha_1\alpha_3^3\alpha_6\alpha_9 + 8\alpha_1\alpha_3^2\alpha_8\alpha_9^2 + 24\alpha_1\alpha_3\alpha_6\alpha_9^3 - 32\alpha_1\alpha_8\alpha_9^4 + 4\alpha_2\alpha_3^2\alpha_6\alpha_9^2 - 8\alpha_2\alpha_3\alpha_8\alpha_9^3$$

$$+ 32\alpha_2\alpha_6\alpha_9^4 + \alpha_6^2\alpha_3^4 - 4\alpha_3^3\alpha_6\alpha_8\alpha_9 - 4\alpha_3^2\alpha_6^2\alpha_9^2 + 4\alpha_3^2\alpha_8^2\alpha_9^2 - 8\alpha_3\alpha_5\alpha_9^3 + 32\alpha_4\alpha_9^4 + 32\alpha_7\alpha_9^4),$$

$$\varphi_6 = \frac{1}{4\alpha_9\sqrt{\Delta_1}}((2\alpha_2\alpha_9 - \alpha_3\alpha_8)\sqrt{\Delta_1} + 8\alpha_1\alpha_9^2 - 2\alpha_2\alpha_3\alpha_9 + \alpha_3^2\alpha_8 - 4\alpha_3\alpha_6\alpha_9),$$

$$\varphi_7 = \frac{\alpha_9}{\Delta_1\sqrt{\Delta_1}}((\alpha_3\alpha_8 - 2\alpha_2\alpha_9)\sqrt{\Delta_1} + 8\alpha_1\alpha_9^2 - 2\alpha_2\alpha_3\alpha_9 + \alpha_3^2\alpha_8 - 4\alpha_3\alpha_6\alpha_9),$$

$$\varphi_8 = \frac{1}{2\sqrt{\Delta_1}}(-\alpha_3 + \sqrt{\Delta_1}), \quad \varphi_9 = \frac{\alpha_9}{\Delta_1}(-\alpha_3 - \sqrt{\Delta_1}),$$

$$\varphi_{10} = \frac{1}{\alpha_9\Delta_1}(2\alpha_1\alpha_3^2\alpha_9 - 16\alpha_1\alpha_9^3 - 4\alpha_2\alpha_3\alpha_9^2 - \alpha_3^3\alpha_6 + 2\alpha_3^2\alpha_8\alpha_9 + 8\alpha_2\alpha_3\alpha_9^2).$$

Table 1. Existence and local stability of all equilibriums.

Equilibrium Points	Existence	Stability	Conditions
$E_1^+ = (0, 0, \frac{-\alpha_3+\sqrt{\Delta}}{2\alpha_9})$	$\Delta > 0$ and $\alpha_9 \neq 0$	Unstable	Always
$E_1^- = (0, 0, \frac{-\alpha_3-\sqrt{\Delta}}{2\alpha_9})$	$\Delta > 0$ and $\alpha_9 \neq 0$	Asymptotically stable	$\frac{2\alpha_9\sqrt{\Delta}+\sqrt{\Delta}+\alpha_3}{2\alpha_9} > 0$ and $(2\alpha_9\sqrt{\Delta} + \sqrt{\Delta} + \alpha_3)(\alpha_9\sqrt{\Delta} + \Delta + 2\alpha_9) > 4\alpha_9^2\sqrt{\Delta}$
$E_2 = (0, 0, -\frac{\alpha_0}{\alpha_3})$	$\Delta > 0$ and $\alpha_9 = 0$	Unstable	$\alpha_3 > 0$
		Asymptotically stable	$\alpha_3 < 0$, $\alpha_0 < \alpha_3^2$ and $(\alpha_0 - \alpha_3^2)(1 - \alpha_0) < -\alpha_3^2$
$E_3 = (0, 0, -\frac{\alpha_3}{2\alpha_9})$	$\Delta = 0$ and $\alpha_9 \neq 0$	Unstable	$\frac{\alpha_3}{\alpha_9} \neq 0$

The set below represents the one-dimensional local center manifold of system (19) in the vicinity of the origin:

$$W^c = \{(u, v, w) \in \mathbb{R}^3 : v = h_1(u), w = h_2(u),$$
$$|u| < 1, \text{ with } h_1(0) = Dh_1(0)$$
$$= h_2(0) = Dh_2(0) = 0\}.$$

From the Taylor expansion near the origin,

$$h_1(u) = \xi_1 u^2 + O(3) \quad \text{and} \quad h_2(u) = \xi_2 u^2 + O(3),$$

$\xi_1 = 0$ and $\xi_2 = 0$ are obtained. The vector field is restricted to the center manifold, which can be expressed by the following equation:

$$\dot{u} = \alpha_9 u^2 + O(3). \tag{20}$$

When $\alpha_9 \neq 0$, then $u = 0$ is unstable for Eq. (20). Therefore, the equilibrium point E_3 is unstable [see Fig. 3(b)]. ∎

The results obtained in this section can be summarized in Table 1.

4. Bifurcation Analysis

Parameters play a crucial role in the formulation of differential equations. The qualitative behavior of a system's solutions can exhibit significant variations based on the specific values assigned to its parameters. In general terms, a differential system can be described as undergoing a bifurcation when its trajectory structure changes as a parameter, denoted by μ, crosses a specific value, μ_0. This can be expressed in the context of a system represented by the equation:

$$\dot{X} = f(X, \mu) = AX + F(X, \mu). \tag{21}$$

Here, X is a variable in $\mathbb{R}^3$, AX represents the linear component of the system, F is a nonlinear analytic function and $\mu \in \mathbb{R}^k$ is a parameter. Simply put, at the bifurcation value, the system experiences a change in the quantity and/or stability of its equilibria. Bifurcations refer to transformative changes that occur in the solution curves of a dynamical system when specific parameter values, known as bifurcation values, vary [Muñoz-Alicea, 2011]. The scientific term "bifurcation" is commonly used to describe substantial and qualitative alterations in the stability of solution curves within nonlinear dynamical systems [Moiola & Chen, 1996]. This section focuses on the analysis of both Hopf and Saddle-Node bifurcations of system (1), with consideration given to their conditions for occurrence.

4.1. Saddle-Node bifurcation

A Saddle-Node bifurcation denotes a significant juncture or a change in the behavior of a dynamical system when a parameter undergoes variation. During a Saddle-Node bifurcation, as the parameter gradually changes, two equilibrium points of the system converge and annul each other, resulting in the disappearance of these equilibria. This critical parameter value brings about a qualitative shift in the system's behavior, often resulting in a transition from a stable equilibrium to an unstable state or vice versa [Perko, 2013; Kuznetsov, 2006].

Theorem 1 [Sotomayor Perko, 2013]. *Consider system (21) and let there is a point $E_0 \in \mathbb{R}^n$ such that $f(E_0, \mu) = 0 \, \forall \, \mu$, i.e. E_0 is an equilibrium point of the system. Moreover, if $\mu = \mu_0$ assume the following condition satisfies*:

(I) *The Jacobian matrix $J = Df(E_0, \mu_0)$ has a zero eigenvalue with an eigenvector v and J^T has an eigenvector ω corresponding to zero eigenvalue. Furthermore, J has k eigenvalues with negative real parts and has $n-k-1$ eigenvalues with positive real parts, where $0 \leq k \leq n-1$;*

(II) $\omega^T f_\mu(E_0, \mu_0) \neq 0$;

(III) $\omega^T (D_x^2 f_\mu(E_0, \mu_0)(v, v)) \neq 0$.

Then, system (21) exhibits a Saddle-Node bifurcation at the equilibrium E_0 as μ passes through $\mu = \mu_0$.

Proposition 2. *For system (1), a Saddle-Node bifurcation occurs at $E_3 = (0, 0, -\frac{\alpha_3}{2\alpha_9})$ as the parameter α_0 passes through $\alpha_0 = \frac{\alpha_3^2}{4\alpha_9}$.*

Proof. By linearizing around E_3 with $\alpha_0 = \frac{\alpha_3^2}{4\alpha_9}$, the Jacobian matrix of system (1) is given by

$$J = \begin{pmatrix} 0 & 1 & 0 \\ -1 & -\frac{\alpha_3}{2\alpha_9} & 0 \\ \alpha_1 - \frac{\alpha_3 \alpha_2}{2\alpha_9} & \alpha_2 - \frac{\alpha_3 \alpha_8}{2\alpha_9} & 0 \end{pmatrix},$$

and the characteristic equation is given by

$$\lambda \left(\lambda^2 + \frac{\alpha_3}{2\alpha_9} \lambda + 1 \right) = 0.$$

It has a simple zero with two solutions having nonzero real parts. The following vectors:

$$\upsilon = \begin{pmatrix} 0 \\ 0 \\ 1 \end{pmatrix} \quad \text{and}$$

$$\omega = \begin{pmatrix} \dfrac{2\alpha_1\alpha_3\alpha_9 - 4\alpha_2\alpha_9^2 - \alpha_3^2\alpha_6 + 2\alpha_3\alpha_8\alpha_9}{4\alpha_9^2} \\ \dfrac{2\alpha_1\alpha_9 - \alpha_3\alpha_6}{2\alpha_9} \\ 1 \end{pmatrix},$$

are eigenvectors of the Jacobian matrices J and J^T corresponding to $\lambda_1 = 0$, respectively. According to Theorem 1, we have

$$\omega^T f_{\alpha_0}\left(E_3, \frac{\alpha_3^2}{4\alpha_9}\right) = 1 \neq 0,$$

$$\omega^T\left(D_x^2 f\left(E_3, \frac{\alpha_3^2}{4\alpha_9}\right)\right) = 2\alpha_9 \neq 0.$$

Therefore, when the parameter α_0 crosses the value $\alpha_0 = \frac{\alpha_3^2}{4\alpha_9}$, system (1) undergoes a Saddle-Node bifurcation at the equilibrium $E_3 = (0, 0, -\frac{\alpha_3}{2\alpha_9})$. ∎

4.2. *Hopf bifurcation*

In recent years, there has been significant research on the Hopf bifurcation of well-known chaotic systems, making it one of the most actively explored subjects in the field [Wouapi *et al.*, 2019; Wang *et al.*, 2023; Kyaw *et al.*, 2023; Guo *et al.*, 2023; Dias & Mello, 2013; Zhang *et al.*, 2013; Wu & Fang, 2015; Van Gorder & Choudhury, 2011; Llibre & Pessoa, 2015; Yu & Zhang, 2003; Wang, 2009; Sun *et al.*, 2006]. Additionally, the Hopf bifurcation is a common phenomenon linked to the emergence or vanishing of limit cycles around an equilibrium point. What sets this bifurcation apart from other common types, such as Saddle-Node, transcritical or pitchfork, is its uniqueness in two aspects. The first aspect is that the Hopf bifurcation cannot occur in one dimension; it requires a minimum dimensionality of two. The second aspect is related to the appearance or disappearance of periodic solutions [Sarmah *et al.*, 2015]. The Hopf bifurcation represents the most straightforward mechanism through which limit cycles can emerge from an equilibrium point. Several techniques can be employed to investigate it, including bifurcation formulas [Wouapi *et al.*, 2019; Sarmah *et al.*, 2015; Akhter, 2024; Sotomayor *et al.*, 2007], Lyapunov quantities [Salih, 2015; Salih & Mohammed, 2022] and focus quantities [Sang, 2021; Sang & Huang, 2017].

Now, let's mention the main condition for the occurrence of the Hopf bifurcation. Suppose that system (21) has an equilibrium (E_0, μ_0) at which the following properties are satisfied:

(I) The Jacobian matrix $J = Df(E_0, \mu_0)$ has a simple pair of pure imaginary eigenvalues $\lambda(\mu)$ and $\bar{\lambda}(\mu)$, while the other eigenvalue has a nonzero real part.

(II) $\frac{d\mathrm{Re}(\lambda(\mu))}{d\mu}\big|_{\mu=\mu_0} \neq 0.$

Then, system (21) has a Hopf bifurcation at the equilibrium (E_0, μ_0) [Guckenheimer & Holmes, 2013].

An explanation is provided for the sufficient condition that leads to the occurrence of the first condition of Hopf bifurcation in system (21). Let us assume that the characteristic polynomial at the origin is given by

$$P(\lambda) = \lambda^3 - T\lambda^2 - K\lambda - D, \qquad (22)$$

where T, K and D represent the trace, sum of diagonal minors and determinant of the Jacobian matrix of system (21) at the origin, respectively. Then, the Hopf bifurcation occurs at the origin if and only if

$$TK + D = 0, \quad K < 0 \quad \text{and} \quad T \neq 0. \quad (23)$$

The bifurcation of multiple limit cycles from a focus is closely tied to the stability of the focus itself. Andronov [1971] introduced a set of numbers called focal values, denoted as η_{2i} $(i = 1, 2, 3, \ldots)$, to describe this phenomenon. Here, the Lyapunov quantity technique is utilized to assess the cyclicity in the three-dimensional system. The technique involves introducing a function of the form

$$F(x, y, z) = x^2 + y^2 + \sum_{k=3}^{\infty} F_k(x, y, z; \mu), \quad (24)$$

where F_k represents a polynomial in x, y and z of degree k and the coefficients of F_k satisfy

$$\chi(F) = \eta_2 r^2 + \eta_4 r^4 + \eta_6 r^6 + \cdots + \eta_{2i} r^{2i} + \cdots, \quad (25)$$

where $r^2 = x^2 + y^2$ or x^2 or y^2 or $(x^2 + y^2)^2$ or other suitable forms. The vector field χ corresponds to the canonical form of the system. The

η_{2i} values (where $i = 1, 2, 3, \ldots$) represent polynomials in the system's parameter μ and are referred to as the ith Lyapunov quantity or focal values. If $\eta_2 = \eta_2 = \eta_2 = \cdots = \eta_{2k} = 0$, but $\eta_{2k+1} \neq 0$, we classify the origin as a fine focus of order k. In such cases, the perturbation of the system can result in the bifurcation of a maximum of k limit cycles from the origin. The exact number of limit cycles can be determined by considering the independence of the Lyapunov quantities. To delve into this technique further, consider [Andronov, 1971; Blows & Lloyd, 1984; Dumortier *et al.*, 2006; Lu & Luo, 2002; Wang, 1991] for more detailed information.

4.2.1. *Hopf bifurcation conditions*

The main focus of this section is to determine the conditions for the occurrence of Hopf bifurcation.

Proposition 3. *If α_0 crosses the critical value of $\alpha_0 = 0$, subject to the conditions that $\alpha_3 \neq -2\alpha_9\sqrt{\Delta} - \sqrt{\Delta}$ and $\frac{\alpha_9\sqrt{\Delta} - \sqrt{\Delta} - 2\alpha_9}{2\alpha_9} < 0$*

then system (1) undergoes a Hopf bifurcation at the equilibrium point $E_1^+(0, 0, \frac{-\alpha_3+\sqrt{\Delta}}{2\alpha_9})$ (for $E_1^-(0, 0, \frac{-\alpha_3-\sqrt{\Delta}}{2\alpha_9})$ is similar by changing the sign of Δ) where $\Delta = \alpha_3^2 - 4\alpha_9\alpha_0 > 0$ and $\alpha_9 \neq 0$.

Proof. By using the linear transformation $x_3 \to x_3 + \frac{-\alpha_3+\sqrt{\Delta}}{2\alpha_9}$, the equilibrium point $E_1^\pm$ is shifted to the origin and system (1) becomes

$$\dot{x}_1 = x_2,$$

$$\dot{x}_2 = -x_1 + \varphi_1 x_2,$$

$$\dot{x}_3 = \alpha_0 + \alpha_1 x_1 + \alpha_2 x_2 + \alpha_3 \varphi_1 + \alpha_4 x_1^2 \qquad (26)$$

$$\quad + \alpha_5 x_1 x_2 + \alpha_6 \varphi_1 x_1 + \alpha_7 x_2^2 + \alpha_8 \varphi_1 x_2$$

$$\quad + \alpha_9 \varphi_1^2,$$

where $\varphi_1 = x_3 + \frac{-\alpha_3+\sqrt{\Delta}}{2\alpha_9}$. For the given system, at the origin, the Jacobian matrix and its characteristic equation are defined as follows, respectively:

$$J = \begin{pmatrix} 0 & 1 & 0 \\ 0 & 0 & 1 \\ \sqrt{\Delta} & \alpha_2 + \dfrac{\alpha_5(-\alpha_1 + \sqrt{\Delta})}{2\alpha_4} & \alpha_3 + \dfrac{\alpha_6(-\alpha_1 + \sqrt{\Delta})}{2\alpha_4} \end{pmatrix},$$

$$f(\lambda, \alpha_0) = \lambda^3 - \frac{2\alpha_9\sqrt{\Delta} + \sqrt{\Delta} - \alpha_3}{2\alpha_9}\lambda^2 - \frac{\alpha_3\sqrt{\Delta} - \sqrt{\Delta} - 2\alpha_9}{2\alpha_9}\lambda - \sqrt{\Delta} = 0. \qquad (27)$$

Upon comparing the aforementioned characteristic equation with Eq. (22), the subsequent values for T, K and D are determined: $T = \frac{2\alpha_9\sqrt{\Delta} + \sqrt{\Delta} - \alpha_3}{2\alpha_9}$, $K = \frac{\alpha_3\sqrt{\Delta} - \sqrt{\Delta} - 2\alpha_9}{2\alpha_9}$ and $D = \sqrt{\Delta}$. The characteristic polynomial (27) exhibits a Hopf point, characterized by two nonzero purely imaginary solutions, only when its coefficients fulfill conditions (23). Then, when

- $T \neq 0$, it implies that $\alpha_3 \neq -2\alpha_9\sqrt{\Delta} - \sqrt{\Delta}$;

- $K < 0$, it implies that $\frac{\alpha_9\sqrt{\Delta} - \sqrt{\Delta} - 2\alpha_9}{2\alpha_9} < 0$;

- $TK + D = 0$, it implies that $(4\alpha_0\alpha_9^2 - \alpha_3^2\alpha_9 + 2\alpha_0\alpha_9 - \alpha_9 - \alpha_3^2)\sqrt{\Delta} - 4\alpha_0\alpha_3\alpha_9^2 - \alpha_3^3\alpha_9 - 4\alpha_0\alpha_9 + \alpha_3\alpha_9 - \alpha_3^3 = 0$.

The conditions mentioned above lead to $\alpha_0 = 0$ and $\alpha_3 > 0$. Consequently, the characteristic equation (27) possesses a nonzero eigenvalue α_0 along with a pair of purely imaginary eigenvalues $\pm i$.

To confirm the transversality condition, the derivative of the complex eigenvalue $\lambda(\alpha_0)$ with respect to α_0 can be determined for the equilibrium point using the implicit function theorem, as follows:

$$\frac{d\lambda}{d\alpha_0} = -\frac{\dfrac{\partial f}{\partial \alpha_0}}{\dfrac{\partial f}{\partial \lambda}} = \frac{2\alpha_9((2\alpha_9 + 1)\lambda^2 + (\alpha_3 - 2\sqrt{\Delta})\lambda + 2\alpha_9)}{\sqrt{\Delta}(6\alpha_9\lambda^2 + (2\alpha_3 - (4\alpha_9 + 2)\sqrt{\Delta})\lambda - \alpha_3\sqrt{\Delta} + \Delta + 2\alpha_9)}. \qquad (28)$$

Substituting $\alpha_0 = 0$ and $\lambda = i$ into Eq. (28), we obtain

$$\left.\frac{d\mathrm{Re}(\lambda_{1,2})}{d\alpha_0}\right|_{\{\alpha_0=0,\lambda=i\}} = \frac{1}{3\alpha_3} \neq 0. \qquad (29)$$

This indicates that the transversality condition has been fulfilled. Thus, Hopf bifurcation takes place at $\alpha_0 = 0$. ∎

Proposition 4. *For system (1), Hopf bifurcation occurs at the equilibrium point $E_2 = (0, 0, -\frac{\alpha_0}{\alpha_3})$; $\alpha_3 \neq 0$ when $\alpha_0 = 0$.*

Proof. By applying a linear transformation $x_3 = x_3 - \frac{\alpha_0}{\alpha_3}$, we shift the equilibrium point E_2 to the origin $E_{20} = (0, 0, 0)$, thereby transforming system (1) into the following:

$$\dot{x}_1 = x_2,$$
$$\dot{x}_2 = -x_1 + \varphi_2 x_2,$$
$$\dot{x}_3 = \alpha_0 + \alpha_1 x_1 + \alpha_2 x_2 + \alpha_3 \varphi_2 \qquad (30)$$
$$\quad + \alpha_4 x_1^2 + \alpha_5 x_1 x_2 + \alpha_6 \varphi_2 x_1 + \alpha_7 x_2^2$$
$$\quad + \alpha_8 \varphi_1 x_2 + \alpha_9 \varphi_2^2,$$

where $\varphi_2 = x_3 - \frac{\alpha_0}{\alpha_3}$. From (30), the Jacobian matrix at the origin is

$$J = \begin{pmatrix} 0 & 1 & 0 \\ -1 & -\frac{\alpha_0}{\alpha_3} & 0 \\ \alpha_1 - \frac{\alpha_0 \alpha_6}{\alpha_3} & \alpha_2 - \frac{\alpha_0 \alpha_8}{\alpha_3} & \alpha_3 \end{pmatrix},$$

and its characteristic equation is

$$\lambda^3 - \frac{\alpha_0 - \alpha_3^2}{\alpha_3}\lambda^2 - (1 - \alpha_0)\lambda - \alpha_3 = 0. \quad (31)$$

Since $\alpha_0 = 0$, Eq. (31) changes into

$$(\lambda^2 + 1)(\lambda - \alpha_3) = 0. \qquad (32)$$

Hence, Eq. (32) exhibits a pair of conjugate roots that are purely imaginary, namely $\lambda_{1,2} = \pm i$ and a real root $\lambda_3 = \alpha_3$. Thus, we can choose α_0 as the bifurcation parameter and the critical value is $\alpha_0 = 0$. According to Eq. (31), we have

$$\lambda'(\alpha_0) = \frac{\lambda^2 - \alpha_3 \lambda}{3\alpha_3 \lambda^2 + (2\alpha_0 - 2\alpha_3^2)\lambda + \alpha_3(1 - \alpha_0)}.$$

Hence, $\mathrm{Re}(\lambda'(\alpha_0))|_{\lambda=i} = -\frac{1}{2\alpha_3}$ and $\mathrm{Im}(\lambda'(\alpha_0))|_{\lambda=i} = 0$. Since λ_1 and λ_2 are a conjugate pair $(\lambda_1(\alpha_0) = \bar{\lambda}_2(\alpha_0))$, $\mathrm{Re}(\lambda_1'(\alpha_0))|_{\lambda=i} \neq 0$, $\mathrm{Im}(\lambda_1(\alpha_0)) \neq 0$ and

$\mathrm{Re}(\lambda_3(\alpha_0)) = \alpha_3 \neq 0$. Then, a Hopf bifurcation occurs at $E_2 = (0, 0, -\frac{\alpha_0}{\alpha_3})$. ∎

4.2.2. *Multiple Hopf bifurcations*

To analyze the cyclicity of the three-dimensional system (1), we utilize the Lyapunov quantities technique referenced in [Salih, 2015; Salih & Mohammed, 2022]. However, due to the computational complexity involved in calculating Lyapunov quantities, certain parameters are held constant.

First, we investigate the number of limit cycles that can bifurcate from a Hopf point $E_1^+(0, 0, \frac{-\alpha_3+\sqrt{\Delta}}{2\alpha_9})$. We carried out this investigation by fixing certain parameters, such as $\alpha_1 = \alpha_2 = \alpha_3 = \alpha_6 = \alpha_7 = \alpha_8 = \alpha_9 = 1$. Thus, system (26) becomes

$$\dot{x}_1 = x_2,$$
$$\dot{x}_2 = -x_1 + \varphi_3 x_2,$$
$$\dot{x}_3 = \alpha_0 + x_1 + x_2 + \varphi_3 + \alpha_4 x_1^2 + \alpha_5 x_1 x_2 \qquad (33)$$
$$\quad + \varphi_3 x_1 + x_2^2 + \varphi_3 x_2 + \varphi_3^2,$$

where $\varphi_3 = \frac{-1+\sqrt{1-4\alpha_0}}{2}$. The equation that describes the characteristics of the linearized system (33) at the origin is expressed as follows:

$$\lambda^3 - \frac{1 - 3\sqrt{1-4\alpha_0}}{2}\lambda^2 - \frac{3 - 4\alpha_0 - \sqrt{1-4\alpha_0}}{2}\lambda$$
$$\quad - \sqrt{1-4\alpha_0} = 0. \qquad (34)$$

When $\alpha_0 = 0$, Eq. (34) possesses a pair of conjugate roots that are purely imaginary, namely $\lambda_{1,2} = \pm i$, along with a nonzero root $\lambda_3 = 1$. Using Eq. (34) and applying the implicit function theorem, we compute

$$\left.\frac{d\mathrm{Re}(\lambda_1)}{d\alpha_0}\right|_{\{\alpha_0=0,\lambda=i\}} = -\frac{1}{2} \neq 0.$$

Therefore, the transversality condition for the Hopf bifurcation at $\alpha_0 = 0$ is confirmed. Thus, a Hopf bifurcation occurs at the origin equilibrium when the parameter $\alpha_0 = 0$.

In order to study the cyclicity, the Lyapunov quantities technique is used. By the following linear transformation,

$$x_1 = u, \quad x_2 = -v, \quad x_3 = v + w,$$

system (33) transformed into the following canonical form:

$$\dot{u} = -v,$$
$$\dot{v} = u + vw + v^2, \qquad (35)$$
$$\dot{w} = w + (1 - \alpha_5)uv + uw + \alpha_4\, u^2 + w^2.$$

To examine the number of bifurcated limit cycles from the equilibrium point, we define the following Lyapunov function:

$$F(u, v, w) = u^2 + v^2 + \sum_{k=3}^{n}\sum_{j=0}^{k}\sum_{i=0}^{j} C_{i,j-i,k-j}$$
$$\times u^i v^{j-i} w^{k-j},$$

such that

$$\chi(F) = \eta_2(u^2+v^2)^2 + \eta_4(u^2+v^2)^4 + \eta_6(u^2+v^2)^6$$
$$+ \cdots + \eta_{2i}(u^2+v^2)^{2i} + \cdots, \qquad (36)$$

where χ denotes the vector field of system (33). Equation (36) is solved and a subsequent set of mutually independent Lyapunov quantities is derived using the technique described in [Salih, 2015] and the computer algebra package MAPLE.

$$\eta_1 = 0,$$
$$\eta_2 = \frac{1}{20}(2 - 9\alpha_4 - 2\alpha_5),$$
$$\eta_3 = \frac{1}{800}(485\alpha_4 + 340\alpha_5 - 458\alpha_4^2$$
$$- 183\alpha_4\alpha_5 - 42\alpha_5^2),$$
$$\eta_4 = \frac{1}{97920000}(-105930441\alpha_4^3 - 51928074\alpha_4^2\alpha_5$$
$$- 106705482\alpha_4^2 - 15466437\alpha_4\alpha_5^2$$
$$+ 61471688\alpha_4\alpha_5 - 210386861\alpha_4 - 1534302\alpha_5^3$$
$$+ 4866802\alpha_5^2 - 128656278\alpha_5 + 125323778).$$

The origin in system (33) is classified as a weak focus of order three if and only if the following conditions are met:

$$\alpha_4 = \frac{2}{9}(1 - \alpha_5) \quad \text{and} \quad \alpha_5 = \frac{862}{97}.$$

Now, the Jacobian determinant of the functions $[\eta_2, \eta_3]$ with respect to α_4 and α_5 at $\alpha_4 = \frac{4}{5}(1 - \alpha_5)$

and $\alpha_5 = \frac{462}{97}$ is given by

$$\begin{vmatrix} \dfrac{\partial\eta_2}{\partial\alpha_4} & \dfrac{\partial\eta_2}{\partial\alpha_5} \\[2mm] \dfrac{\partial\eta_3}{\partial\alpha_4} & \dfrac{\partial\eta_3}{\partial\alpha_5} \end{vmatrix} = \frac{-74893}{698400} \neq 0.$$

We observe that at $(\alpha_4, \alpha_5) = (\frac{2}{9}(1 - \alpha_5), \frac{862}{97})$, the fourth Lyapunov quantity is nonzero, with a value of $\eta_4 = \frac{-198846157}{14602768}$ and $\eta_2 = \eta_3 = 0$. By appropriately perturbing the coefficients of the Lyapunov quantities, it is possible for three limit cycles to bifurcate from the origin of system (33) in its vicinity. Thus, based on the aforementioned calculations and Proposition 3, we can derive the following theorem.

Theorem 2. *For system* (1), *under conditions on Proposition 3, three limit cycles can be bifurcated from the equilibrium point* $E_1^+(0, 0, \frac{-\alpha_3 + \sqrt{\Delta}}{2\alpha_9})$ *when the parameter* α_0 *passes through zero.*

Second, we investigate the number of limit cycles that can bifurcate from a Hopf point $E_2 = (0, 0, -\frac{\alpha_0}{\alpha_3})$; $\alpha_3 \neq 0$. This investigation is carried out by fixing certain parameters, such as $\alpha_1 = \alpha_2 = \alpha_3 = \alpha_6 = \alpha_7 = \alpha_8 = 1$. In a similar manner to the proof of Theorem 2, it is straightforward to establish the following theorem.

Theorem 3. *For system* (1), *three limit cycles can be bifurcated from the equilibrium point* $E_2 = (0, 0, -\frac{\alpha_0}{\alpha_3})$; $\alpha_3 \neq 0$ *when* α_0 *passes through zero.*

5. Conclusions

This paper focuses on the analysis of the three-dimensional generalized Nosé–Hoover system. The stability of the system's equilibrium points has been assessed using characteristic equations. Furthermore, the occurrence of Hopf and Saddle-Node bifurcations has been investigated, considering specific parameter conditions. It is shown that Saddle-Node bifurcations occur at the equilibrium point $E_3 = (0, 0, -\frac{\alpha_3}{2\alpha_9})$ as the parameter α_0 passes through $\alpha_0 = -\frac{\alpha_3^2}{4\alpha_9}$. Under specific conditions on the parameters, it is proved that the Hopf bifurcation occurs at the points $E_1^{\pm}$, where the parameter α_0 passes through zero. To explore the system's cyclicity perturbed from the Hopf points, the Lyapunov quantities have been utilized. To manage the computational complexity associated with computing the Lyapunov quantities, certain parameters

have been held constant. As a result, it has been determined that the system can give rise to three limit cycles through Hopf points.

ORCID

Rizgar H. Salih
https://orcid.org/0000-0001-9408-8602

Julien C. Sprott
https://orcid.org/0000-0001-7014-3283

Bashdar M. Mohammed
https://orcid.org/0000-0001-7358-6207

References

Akhter, T. [2024] "Hopf bifurcation in the model of Caginalp for the price of Bitcoin," https://ssrn.com/abstract=4749454.

Andronov, A. A. [1971] *Theory of Bifurcations of Dynamic Systems on a Plane* (Israel Program of Scientific Translations).

Blows, T. & Lloyd, N. [1984] "The number of limit cycles of certain polynomial differential equations," *Proc. R. Soc. Edinb. A*: *Math.* **98**, 215–239.

Cândido, M. R. & Llibre, J. [2018] "Zero-Hopf bifurcations in 3-dimensional differential systems with no equilibria," *Math. Comput. Simul.* **151**, 54–76.

Cang, S., Wang, L., Zhang, Y., Wang, Z. & Chen, Z. [2022] "Bifurcation and chaos in a smooth 3D dynamical system extended from Nosé–Hoover oscillator," *Chaos Solit. Fract.* **158**, 112016.

Deng, B., Duarte, J., Januário, C. & Martins, N. [2023a] "Measures of complexity in Nosé–Hoover oscillator and a possible new chaos generation mechanism," *Appl. Math. Sci.* **17**, 517–534.

Deng, B., Duarte, J., Januário, C. & Martins, N. [2023b] "On the chaotic dynamics of a modified Nosé–Hoover oscillator," *Appl. Math. Sci.* **17**, 615–623.

Dias, F. S. & Mello, L. F. [2013] "Hopf bifurcations and small amplitude limit cycles in Rucklidge systems," *Electron. J. Differ. Equ.* **48**, 1–9.

Dumortier, F., Llibre, J. & Artés, J. C. [2006] *Qualitative Theory of Planar Differential Systems*, Vol. 2 (Springer).

Euler, L. [1744] "De fractionibus continuis dissertatio," *Comment. Acad. Sci. Petropolitanae* **9**, 98–137.

Guckenheimer, J. & Holmes, P. [2013] *Nonlinear Oscillations, Dynamical Systems, and Bifurcations of Vector Fields*, Vol. 42 (Springer Science & Business Media).

Guo, G., Wang, J. & Wei, M. [2023] "Stability and Hopf bifurcation in the general Langford system," *Qual. Theory Dyn. Syst.* **22**, 144.

Hoover, W. G. [1985] "Canonical dynamics: Equilibrium phase-space distributions," *Phys. Rev. A* **31**, 1695–1697.

Hoover, W. G. [2007] "Nosé–Hoover nonequilibrium dynamics and statistical mechanics," *Mol. Simul.* **33**, 13–19.

Kuznetsov, Y. A. [2006] "Saddle-node bifurcation," *Scholarpedia* **1**, 1859.

Kyaw, E. E., Zheng, H. & Wang, J. [2023] "Hopf bifurcation analysis of a phage therapy model," *Commun. Appl. Math. Comput. Sci.* **18**, 87–106.

Li, W., Shi, S. & Yang, S. [2022] "On integrability of the Nosé–Hoover oscillator and generalized Nosé–Hoover oscillator," *Int. J. Geom. Methods Mod. Phys.* **19**, 2250117.

Llibre, J. & Pessoa, C. [2015] "The Hopf bifurcation in the Shimizu–Morioka system," *Nonlin. Dyn.* **79**, 2197–2205.

Llibre, J., Messias, M. & Reinol, A. C. [2021] "Global dynamics and bifurcation of periodic orbits in a modified Nosé–Hoover oscillator," *J. Dyn. Control Syst.* **27**, 491–506.

Lu, Z. & Luo, Y. [2002] "Two limit cycles in three-dimensional Lotka–Volterra systems," *Comput. Math. Appl.* **44**, 51–66.

Mahdi, A. & Valls, C. [2011] "Integrability of the Nosé–Hoover equation," *J. Geom. Phys.* **61**, 1348–1352.

Mehrabbeik, M., Jafari, S. & Sprott, J. C. [2022] "A simple three-dimensional quadratic flow with an attracting torus," *Phys. Lett. A* **451**, 128427.

Messias, M. & Reinol, A. C. [2018] "On the existence of periodic orbits and KAM tori in the Sprott A system: A special case of the Nosé–Hoover oscillator," *Nonlin. Dyn.* **92**, 1287–1297.

Moiola, J. L. & Chen, G. [1996] *Hopf Bifurcation Analysis: A Frequency Domain Approach*, Vol. 21 (World Scientific).

Munmuangsaen, B., Sprott, J. C., Thio, W. J.-C., Buscarino, A. & Fortuna, L. [2015] "A simple chaotic flow with a continuously adjustable attractor dimension," *Int. J. Bifurcation and Chaos* **25**, 1530036.

Muñoz-Alicea, R. [2011] "Introduction to bifurcations and the Hopf bifurcation theorem for planar systems," Technical report, Department of Mathematics, Colorado State University.

Nosé, S. [1984a] "A molecular dynamics method for simulations in the canonical ensemble," *Mol. Phys.* **52**, 255–268.

Nosé, S. [1984b] "A unified formulation of the constant temperature molecular dynamics methods," *J. Chem. Phys.* **81**, 511–519.

Perko, L. [2013] *Differential Equations and Dynamical Systems*, Vol. 7, 3rd edition (Springer Science & Business Media).

Posch, H. A., Hoover, W. G. & Vesely, F. J. [1986] "Canonical dynamics of the Nosé oscillator: Stability, order, and chaos," *Phys. Rev. A* **33**, 4253–4265.

Rech, P. C. [2016] "Quasiperiodicity and chaos in a generalized Nosé–Hoover oscillator," *Int. J. Bifurcation and Chaos* **26**, 1650170.

Salih, R. H. [2015] "Hopf bifurcation and centre bifurcation in three dimensional Lotka–Volterra systems," PhD thesis, Plymouth University.

Salih, R. H. & Mohammed, B. M. [2022] "Hopf bifurcation analysis of a chaotic system," *Zanco J. Pure Appl. Sci.* **34**, 87–100.

Sang, B. & Huang, B. [2017] "Bautin bifurcations of a financial system," *Electron. J. Qual. Theory Differ. Equ.* **2017**, 1–22.

Sang, B. [2021] "Focus quantities with applications to some finite-dimensional systems," *Math. Methods Appl. Sci.* **44**, 464–475.

Sarmah, H. K., Das, M. C. & Baishya, T. K. [2015] "Hopf bifurcation in a chemical model," *Int. J. Innov. Res. Sci. Eng. Technol.* **1**, 23–33.

Sotomayor, J., Mello, L. F. & Braga, D. d. C. [2007] "Bifurcation analysis of the Watt governor system," *Commun. Appl. Math.* **26**, 19–44.

Sprott, J. C., Hoover, W. G. & Hoover, C. G. [2014] "Heat conduction, and the lack thereof, in time-reversible dynamical systems: Generalized Nosé–Hoover oscillators with a temperature gradient," *Phys. Rev. E* **89**, 042914.

Sprott, J. C. [2015] "Strange attractors with various equilibrium types," *Eur. Phys. J. Spec. Top.* **224**, 1409–1419.

Sprott, J. C. [2018] "Ergodicity of one-dimensional oscillators with a signum thermostat," *Comput. Methods Sci. Technol.* **24**, 169–176.

Sun, M., Tian, L. & Yin, J. [2006] "Hopf bifurcation analysis of the energy resource chaotic system," *Int. J. Nonlin. Sci.* **1**, 49–53.

Swinnerton-Dyer, P. & Wagenknecht, T. [2008] "Some third-order ordinary differential equations," *Bull. Lond. Math. Soc.* **40**, 725–748.

Van Gorder, R. A. & Choudhury, S. R. [2011] "Analytical Hopf bifurcation and stability analysis of T system," *Commun. Theor. Phys.* **55**, 609.

Wang, D. [1991] "Mechanical manipulation for a class of differential systems," *J. Symbol. Comput.* **12**, 233–254.

Wang, X. [2009] "Si'lnikov chaos and Hopf bifurcation analysis of Rucklidge system," *Chaos Solit. Fract.* **42**, 2208–2217.

Wang, L. & Yang, X.-S. [2015] "The invariant tori of knot type and the interlinked invariant tori in the Nosé–Hoover oscillator," *Eur. Phys. J. B* **88**, 1–5.

Wang, L. & Yang, X.-S. [2017] "The coexistence of invariant tori and topological horseshoe in a generalized Nosé–Hoover oscillator," *Int. J. Bifurcation and Chaos* **27**, 1750111.

Wang, L. & Yang, X.-S. [2018] "Global analysis of a generalized Nosé–Hoover oscillator," *J. Math. Anal. Appl.* **464**, 370–379.

Wang, H., Wang, S., Gu, Y. & Yu, Y. [2023] "Hopf bifurcation analysis of a two-dimensional simplified Hodgkin–Huxley model," *Mathematics* **11**, 717.

Wouapi, K. M., Fotsin, B. H., Feudjio, K. F. & Njitacke, T. Z. [2019] "Hopf bifurcation, offset boosting and remerging Feigenbaum trees in an autonomous chaotic system with exponential nonlinearity," *SN Appl. Sci.* **1**, 1–22.

Wu, R. & Fang, T. [2015] "Stability and Hopf bifurcation of a Lorenz-like system," *Appl. Math. Comput.* **262**, 335–343.

Yu, Y. & Zhang, S. [2003] "Hopf bifurcation in the Lü system," *Chaos Solit. Fract.* **17**, 901–906.

Zhang, X.-D., Liu, X.-D., Zheng, Y. & Liu, C. [2013] "Chaotic dynamic behavior analysis and control for a financial risk system," *Chin. Phys. B* **22**, 030509.